ASSESSMENT OF THE CONFORMATIONAL PROFILE OF BOMBESIN BY COMPUTATIONAL METHODS

Abel Valverde, Patricia Gomez-Gutierrez and Juan J. Perez*

Dept. of Chemical engineering, ETSEIB; Universitat Politecnica de Catalunya; Av. Diagonal, 647; 08028 Barcelona, Spain

e-mail address: juan.jesus.perez@upc.edu

keywords: bombesin; conformational analysis; molecular dynamics; structure-activity analysis; bioactive peptide

ABSTRACT

In the present work, the results of a computational study aimed at assessing the conformational profile of bombesin are reported. The conformational space of the peptide was sampled by means of a 4μs accelerated molecular dynamics simulation in water, using an explicit solvent model. The results were analyzed using Principal Component Analysis to get essential information on peptide fluctuations, along with cluster analysis to characterize different conformations in the sample. Analysis of the results suggests that the peptide adopts helical structures at the C-terminus that tend to unwind at the end of the peptide chain, since there are many structures exhibiting only two turns of a helix at the central segment of the peptide. In addition, the peptide also adopts hairpin turn structures at the N-terminus. Results of the simulation were confronted with available NMR results in a 2,2,2-trifluoroethanol/water (30% v/v) solution. Distances deduced form NOEs experiments only provide support to the presence of helical conformations that represent the most populated structures in the simulation. The absence of other conformations in the NMR experiments can be explained to be due to the α-helix enhancing nature of the solvent used in the experiments.

INTRODUCTION

Bombesin, a tetradecapeptide with the sequence: Glp[1]-Gln[2]-Arg[3]-Leu[4]-Gly[5]-Asn[6]-Gln[7]-Trp[8]-Ala[9]-Val[10]-Gly[11]-His[12]-Leu[13]-Met[14]-NH_2 (Glp = pyroglutamic acid) was originally isolated from the skin of the European frog *Bombina bombina*[1]. After its discovery, other peptides with high sequence identity like Ranatensin, Alytensin, Phyllolitorin or Litorin among others, were subsequently characterized[2,3]. Members of this family can be classified into three groups according to the sequence of the C-terminus: a first group is comprised by the bombesin related peptides with sequence: Gly-His-Leu-Met-NH_2; a second group is comprised of the litorin-ranatensin related peptides with sequence Gly-His-Phe-Met-NH_2; and a third group comprising the phyllolitorin related peptides with sequence: Gly-Ser-Phe(Leu)-Met-NH_2. Despite these peptides were originally isolated from the skin of diverse amphibians, it was later found that they are also widely distributed in mammals[4]. Specifically, only two peptides of this family have been isolated in mammals until now: Neuromedin B (NMB)[5], a member of the litorin-ranatensin family and the Gastrin-releasing peptide (GRP)[6], a 27 residue long peptide together with its short version retaining full activity, the GPR(18-27) -also known as Neuromedin C (NMC)- that belongs to the bombesin related peptides group. These two peptides have homologous C-terminal segments and share an identical C-terminal heptapeptide.

These peptides are involved in a wide spectrum of biological activities both, in the central nervous system including satiety, control of circadian rhythm, thermoregulation and in peripheral tissues, including stimulation of gastrointestinal hormone release, activation of macrophages and effects on development[7]. Actions of these peptides are mediated through three GPCRs: BB_1, BB_2 and BB_3[8]. Bombesin exhibits nanomolar affinity for the BB_2 receptor and about ten times lower affinity for BB_1, showing no affinity for the BB_3 receptor. In contrast, NMB exhibits nanomolar affinity for BB_1 and about fifty times lower affinity for BB_2 receptor[9]. The BB_3 is considered an orphan receptor, since no endogenous ligand has yet been identified. It is involved in energy balance, glucose homeostasis, control of body weight or tumor growth. Due to the wide spectrum of biological activities mediated by the bombesin receptors, there is a considerable interest in the clinical potential of novel agonist and/or antagonist, particularly in the fight against cancer[10,11]. Also, due to its role in the control of appetite, metabolism, and chronic itching they are interesting targets for drug discovery[12,13]. In order to develop new drugs targeting bombesin receptors, it is necessary a deeper understanding of the structure-activity relationships of these peptides. Specifically, identification of the features of the bioactive conformation is necessary to understand the relative position of key residues involved in recognition and activation[14,15].

In regard to bombesin, it was soon demonstrated that the analog bombesin(6-14) is the shortest peptide sequence retaining full activity[16,17]. Moreover, the synthesis and biological evaluation of diverse peptide analogs soon demonstrated that residues Trp^8 and His^{12} are important for the activity of the peptide[18] and that Met^{14} is key for activity, since its deletion transforms the peptide into a potent antagonist[19]. In addition to identify key residues necessary for the biological activity of bombesin, it is also important to understand the conformational features of the peptide. Concerning its structure, spectroscopy studies including NMR[20-24], Infrared (IR)[25], Circular Dichroism (CD) and Fluorescence spectroscopy[26] with the use of different solvents like water, dimethylsulfoxide (DMSO) or 2,2,2-trifluoroethanol-water mixtures have provided information of the conformational features of bombesin. Specifically, NMR reports in water and DMSO[20-22] describe the structure of bombesin as a random coil. In contrast, NMR experiments of bombesin carried out in a 2,2,2-trifluoroethanol/water mixture (30% v/v)[23,24] report that the C-terminal segment of the peptide ranging from residue 6 to 14 displays a helical conformation, although with residues 11 to 14 less sharply structured. Moreover, it was also concluded that the first two N-terminal residues adopt an extended conformation, while the region between residues 3 and 5 exhibits a great deal of flexibility. IR[25], CD and Fluorescence studies[26] also confirm the adoption of a helical conformation when the peptide is incorporated into lipid environments.

Computational studies addressed to assess the conformational profile of bombesin have been also been reported in the past[27]. Thus, Replica Exchange Molecular Dynamics simulations in implicit solvent showed that the peptide attains a helical structure on the segment bombesin(6-14) with a tendency to unwind at the C-terminus. Moreover, these results also show a frequent occurrence of conformations that bring together the side chains of aromatic residues Trp^8 and His^{12} in close proximity, fact that was considered important to explain the importance of these two residues in peptide binding. However, there still open questions regarding the conformational profile of bombesin like, does the peptide adopt any other significant conformation in addition to the helical one? Or, do residues Trp^8 and His^{12} play a role in the stability of the helical structure? Access to faster computers, as well as to more efficient algorithms permits nowadays to perform thorough samplings of flexible molecules. In the present study, we report the results of a detailed computational study of bombesin in water, using accelerated molecular dynamics (aMD) as sampling technique in explicit solvent. Present results confirm the tendency of the peptide to adopt a helical conformation in the middle and C-terminal segments. In addition, present results also show a less populated conformation where the peptide adopts a hairpin turn structure at the N-terminus of the peptide.

METHODS

The starting structure of the peptide in its extended conformation was generated by means of the LEaP program embedded in the Amber 12 software[28]. Subsequently, the structure was soaked in a rectangular cuboid box of equilibrated TIP3P water molecules[29]. The system, composed by the peptide and 25140 water molecules, was neutralized by the addition of one chloride ion. Conformational sampling was carried out after a 4 μs aMD simulation at 300 K, following the protocol previously proposed by McCammon et al. and implemented in Amber 12[30,31]. Specifically, a biased potential is applied to the total energy and the dihedral torsional energy. The simulation was carried out in the NVT collective using the ff99SB force field[32] at 300K and periodic boundary conditions. A cutoff of 10 Å was used for the calculation of the non-covalent interactions and electrostatic interactions were treated using the PME method. Before starting the aMD simulation, the structure was energy minimized through 2500 steps of the steepest descent method followed by a few iterations using the conjugate gradient algorithm in order to remove possible steric clashes. In a subsequent step the system was heated up to 300K using a 100 ps NVT molecular dynamics (MD) calculation at a rate of 30 K per 10 ps and equilibrated thought 1 ns of NPT MD and 1 ns of NVT MD. At this point a 10 ns NVT MD was performed in order to determine the average potential energy (Ep), the mean dihedral energy (Ed), as well as the parameters αP and αD, necessary for the subsequent aMD simulation. During the simulations, the temperature was kept at 300 K thought the Langevin thermostat with a collision frequency of 2 ps^{-1}. Moreover, the SHAKE algorithm was used in order to constrain all bonds involving hydrogen atoms allowing us to use an integration step of 2 fs. After completion of the aMD calculation, effects due to the energy bias were removed using a ten order Maclaurin series reweighting for each configuration in order to recover a canonical ensemble[30].

RESULTS AND DISCUSSION

The conformational profile of the peptide was assessed using 400,000 structures extracted at regular intervals from the 4 μs aMD trajectory. In order to extract the most relevant information about the flexibility of the peptide, the sample was subjected to Principal Component Analysis (PCA)[35] using the cpptraj module embedded in Amber 12[28]. For this purpose, the 400,000 structures were first superimposed to a structure of reference using the backbone coordinates of the diverse residues without including the N- and the C-terminal ones. Then, the displacements of the backbone atoms in regard to the average structure were used to compute a covariance matrix that was subsequently diagonalized to obtain the set of principal components (PCs) together with

their eigenvalues. Once the PCs were rank ordered according to their eigenvalues, the results showed that the first PC captures 23.2% of the variance of the system; the first two PCs capture 40.8% of the variance and the addition of a third component PC3, capture a variance of 52.8%. The low variance captured by PC1 can be attributed to the large flexibility of the peptide, as found in similar studies[36]. Diverse analysis using different number of snapshots were carried out in the present work to rule out a possible bias in the procedure. In a subsequent step, the 400,000 structures were subjected to cluster analysis using of the average linkage algorithm[37]. For this purpose, the backbone Cα root-mean-square deviation of residues 2-13 was used as a measure for the distance between two conformations. Comparison of the results obtained using a different number of clusters suggested that four clusters was adequate to explain qualitatively the conformational profile of the peptide. Figure 1 depicts pictorially the 400,000 structures in the space defined by the three first components PC1- PC3 and its projection onto the (PC1, PC2) plane with the diverse clusters depicted in different colors. Analysis of the Figure permits to observe that although clusters #1, #3 and #4 are overlapped in the (PC1, PC2) map, they can be partially segregated when three PCs are used. Moreover, even using three PCs there is still some overlap between clusters #1 and #4 due to the similarity of the structures contained in both clusters, as described later.

Analysis of the secondary structure contents of the diverse structures of the different clusters permits to obtain a simplified picture of the conformational features of the structures in each cluster. Figures 2a-d show for each of the clusters the secondary structure adopted by the diverse residues (Y-axis) in each of the structures (X-axis), using a color-coded diagram. Thus, analysis of Figure 2a suggests -considering together helical secondary motifs and turns- that cluster #1 (in red in Figure 1) includes partially helical structures of diverse lengths at the central segment of the peptide. Figure 3a depicts pictorially a representative structure of this cluster (the pdb file of the structure is provided as supplementary material). Analysis of Figure 2b suggests that cluster#2 (in green in Figure 1) contains structures with a hairpin turn conformation at the N-terminus involving residues Gln^{2}-Arg^{3}-Leu^{4}-Gly^{5}-Asn^{6}-Gln^{7}-Trp^{8}-Ala^{9}-Val^{10}. Figure 3b depicts pictorially a representative structure of this cluster (the pdb file of the structure is provided as supplementary material). Analysis of Figure 2c suggest that cluster#3 (in navy blue in Figure 1) contains intermediate structures that exhibit diverse combination of turns, as for example the structure shown in Figure 3c (the pdb file of the structure is provided as supplementary material). Finally, analysis of Figure 2d suggest that cluster#4 (in magenta in Figure 1) contains helical structures

involving residues 6-14, as shown in Figure 3d that are closely related with the structures of cluster#1 (the pdb file of the structure depicted in Figure 3d is provided as supplementary material).

Another interesting result from the representation of the structures in the PCs space is that the density of points provides insight into the preferred conformations visited during the sampling process. Moreover, these points can be associated with the features of the free energy landscape (FEL) of the peptide and consequently, permits to identify low free energy conformations as well as the difference between them[35]. Figure 4 shows the projection of the 400,000 structures onto the PC1 and PC2 using a color code that depicts the density of structures contained in a small square used as probe to analyze the space. Inspection of Figure 4 permits to identify four minima. Minimum #1 is located on cluster#1 at coordinates (6,-2.5) and is the most populated, being representative structure is a partial helix located on the central segment of the peptide similar to the representative structure of cluster#1, as shown in Figure 5a (pdb file is provided as supplementary material). Minimum #2 is located in the region of cluster#2 at coordinates (-9.5,-3), being its representative structure a hairpin turn at the N-terminus involving residues Gln^{2}-Arg^{3}-Leu^{4}-Gly^{5}-Asn^{6}-Gln^{7}-Trp^{8}-Ala^{9}-Val^{10} similar to the representative structure of cluster#2, as shown in Figure 5b (pdb file is provided as supplementary material). The representative structure of minimum #3 located at coordinates (-4.5,-10) can be considered an intermediate structure exhibiting a turn of a helix, as shown in Figure 5c (pdb file is provided as supplementary material). Finally, the representative structure of minimum #4 located at coordinates (-9.5,-9.5) can also be considered as an intermediate structure with diverse turns, as shown in Figure 5d (pdb file is provided as supplementary material). These latter two could be considered as kinetic traps.

Analysis of these results provide an emerging qualitative picture of the conformational profile of bombesin: the peptide attains diverse conformations being the most populated the α-helix involving diverse residues at the central and C-terminus segments. On the one hand, cluster#4 includes a large population of helical structures involving residues Asn^{6}-Gln^{7}-Trp^{8}-Ala^{9}-Val^{10}-Gly^{11}-His^{12}-Leu^{13}-Met^{14} and on the other, there is the large population of partially helical structures included in cluster #1 that exhibit a few turns of a helix, suggesting the relevance of the helical conformation in the conformational profile of the peptide. These results taken together permit to interpret that the peptide is likely to attend helical structures with a tendency to unwind at the C-terminus. These structures correspond to those identified in a previous work of this laboratory[27] and agrees well with the results found in NMR experiments[20]. Moreover, the peptide also adopts hairpin turn conformations involving residues at the N-terminus. The rest of the structures correspond to partially folded structures, some of them very populated.

The presence of helical structures at the C-terminus of the peptide could be associated to the activity of the peptide since bombesin(6-14) is the shortest segment retaining full activity[16,17]. However, there are important structural differences between a α-helix involving residues 6-14 and a partial helix involving a few residues in the middle segment that can be relevant to explain the biological activity of the peptide. Structure-activity studies showed the importance of residues Trp^{8} and His^{12} for the activity of the peptide. This can be interpreted in structural terms that these residues play a role in stabilizing the bioactive conformation of the peptide or alternatively that they are directly involved in the recognition by its receptors. The distribution of the distance between the centers of Trp^{8} and His^{12} side chain aromatic rings monitored along the MD trajectory displayed in Figure 6 shows sample a wide set of distances with a maximum between 8-13 Å. Actually, conformations belonging to cluster#2, cluster#3 and cluster#4 exhibit distances between aromatic rings in this range. In contrast, structures belonging to cluster#1 that are partially helical (Figure 3a) exhibit distances ≤ 7 Å. These type of structures permit the side chains of Trp^{8} and His^{12} to be involved in a quadrupole-quadrupole interaction stabilizing the conformation[38]. Actually, side chain-side chain interactions compensate the loss of helicity at the C-terminus in this type of structures explaining why this conformation is the most populated structure in the sampling, representing minimum #1 on the FEL. The importance of adoption of a partial helix at the middle segment for receptor recognition is further reinforced from the results of activity exhibited by diverse bombesin analogs that incorporate turn mimetics in substitution of residues Val^{10}-Gly^{11}[39].

The peptide also adopts hairpin turn conformations at the N-terminus involving residues Gln^{2}-Arg^{3}-Leu^{4}-Gly^{5}-Asn^{6}-Gln^{7}-Trp^{8}-Ala^{9}-Val^{10} (Figure 3b). Actually, the structure is stabilized by hydrogen bonds between the amide hydrogen of Leu^{4} and the carbonyl oxygen of Gln^{7} adopting a reverse type II β-turn and between the carbonyl oxygen of Gln^{2} and the amide hydrogen of Val^{10} that stabilizes the hairpin. This structure corresponds to minimum M2 and it is quite abundant in cluster#2. In these structures the side chains of Trp^{8} and His^{12} do not interact since distances are longer than 10 Å, although we cannot rule out that may be relevant for receptor recognition. An interesting feature of these structures is that one face of the structure aligns side chains of hydrophobic residues, whereas the other face involves polar side chains. This structure is very likely to be adopted by the peptide in lipid-aqueous interfaces. In the FEL there are other two minima represent intermediate structures and can be considered as kinetic traps.

Results of the sampling can be contrasted with the results derived from NMR studies in 2,2,2-trifluoroethanol/water mixture (30% v/v)[23,24]. Specifically, the intensity of the signals obtained from Nuclear Overhauser Effect (NOE) experiments, which stem from cross-relaxation between proton

pairs in NMR experiments are related to the distance between the protons involved, permitting a direct comparison with the results of the molecular dynamics trajectory[33]. According to the literature[34], strong NOE peaks correspond to proton-proton distances in the interval 1,8-2,7 Å; medium NOE peaks in the interval 1,8-3,3 Å, weak NOE peaks in the interval 1,8-5,0 Å and very weak in the interval 1.8-6.0 Å.

Figure 7 shows in orange the distance intervals derived from NOEs experiments according to their intensity, along with the distance intervals sampled by the peptide during the simulation. Inspection of Figure 7 shows that all distance intervals derived from NMR experiments are sampled during the simulation, although during the sampling process the peptide also explores alternative distances that are not detected in the experiments. In order to characterize the structures compatible with the distances derived from NMR experiments, Figures 8a-d shows the same diagram of Figure 6 depicting distances from the set of structures embedded in the square defining each of the minima in the FEL. As can be seen, structures representing minimum M1 (Figure 8a) fit better, although none of the structures completely fulfill the distances derived from NOEs experiments. In other to understand better the features of the experimental structure, we measured the corresponding distances on the representative structures of the different clusters (Figures 3a-d). Interestingly, the representative structure of cluster#4 (Figure 3d) fits the best, except for the N-terminus residues, clearly indicating that in the structure derived from NMR all residues are in a helical conformation. In order to conceal the results from the simulation and from NMR experiments, it is necessary to consider that a peptide in solution is flexible enough to adopt diverse conformations, although in this case, the α-helix is a very populated conformation. On the other hand, the helix enhancing nature of the 2,2,2-trifluoroethanol may bias the experiments, inducing more structured conformations and consequently, increasing the population of helical conformations determined experimentally[40].

From a structure-activity perspective, since the segment bombesin(6-14) is known to retain full activity, helical structures located in the middle and C-terminal segments should be considered relevant for peptide recognition. Moreover, experimental results indicate that Met^{14} is key for receptor activation and that Trp^{8} and His^{12} are relevant for receptor recognition. These results are compatible with a binding mode of bombesin into its receptor through the C-terminus, in such a way that the peptide adopts a helical structure. This permits residue Met^{14} to be the most deeply inserted in connection with its role to be involved in activation[41].

In order to understand the type of helical structure adopted by the peptide when bound to its receptor, it is important to analyze the geometries sampled by the side chains of Trp^{8} and His^{12}.

Distances between the centers of the two aromatic moieties of the respective side chains range from 5 Å to more than 13 Å suggesting that the peptide is quite flexible. Distances more frequently sampled correspond to helical structures and hairpin turns, whereas lower distances correspond to structures of cluster#1 that exhibit a partial helical structure in the middle segment. In these latter structures, the side chains of Trp^{8} and His^{12} are involved in a quadrupole-quadrupole interactions that permit to compensate the loss of helicity of the C-terminus segment explaining the large population sampled. Accordingly, there are two possible binding modes. In one, the peptide adopts a partial helical structure stabilized by the side chains of Trp^{8} and His^{12} that permits the side chains of the rest of the C-terminus residues to adopt a conformation suitable for binding. In the other, the peptide adopts a helix, where the side chains of Trp^{8} and His^{12} do not interact, but adopt a distance suitable for binding to specific residues of the receptor. Unfortunately, the information available does not permit to discard any of the two hypothesis. Further investigations involving modeling of the bombesin receptors are necessary to rule out one of the hypothesis.

CONCLUSIONS

The conformational profile of bombesin was assessed in the present work through a computational study. Specifically, a 4μs accelerated molecular dynamics trajectory was used to sample the conformational space. Analysis of the trajectory was carried out by means of Principal Component Analysis that permitted to extract the essential information of the fluctuations of the peptide complemented by cluster analysis that permitted to classify the diverse conformations sampled in different subsets.

The analysis of the sampling reveals the tendency of the peptide to adopt helical structures at the C-terminus of the peptide as the most populated conformation. More specifically, the peptide adopts a α-helix conformation involving residues Asn^{6}-Gln^{7}-Trp^{8}-Ala^{9}-Val^{10}-Gly^{11}-His^{12}-Leu^{13}-Met^{14} as well as partially helical structures involving two or three helix turns at the central segment of the peptide, being these latter more abundant. The coexistence of these two type of helical conformations can be interpreted considering that the peptide exhibits a α-helix at the C-terminus that tends to unwind in its last residues. In addition, the peptide adopts hairpin structures at the N-terminus involving residues Gln^{2}-Arg^{3}-Leu^{4}-Gly^{5}-Asn^{6}-Gln^{7}-Trp^{8}-Ala^{9}-Val^{10}. This structure permits to obtain a structure with one side hydrophilic and the opposite hydrophobic. These two structures appear as minima in the FEL of the peptide in this work. The rest of structures can be considered as intermediate structures. Interestingly, there are two of the structures that appear very populated in the FEL and can be considered as kinetic traps. These results agree well with the conclusions of previous NMR experiments carried out in 2,2,2-trifluoroethanol.

The features of the bombesin structure sketched in this work permits to speculate that the peptide binds into its receptor through the C-terminus, in such a way that the peptide adopts a helical structure. This permits residue Met^{14} to be the most deeply inserted in connection with its role to be involved in activation.

REFRENCES

1. A. Anastasi, V. Erspamer, and M. Bucci, Isolation and structure of bombesin and alytesin, 2 analogous active peptides from skin of European amphibians bombina and alytes. Experientia. 27 (1971) 166-167.
2. V. Erspamer and P. Melchiorri, Active polypeptides - from amphibian skin to gastrointestinal-tract and brain of mammals. Trends Pharmacol. Sci. 1 (1980) 391-395.
3. R.T. Jensen and T.W. Moody, Bombesin peptides (cancer). In: Hand-book of biologically active peptides. A.J. Kastin, editor, Elsevier, Amsterdam, 2013, pp. 506–511.
4. H. Ohki-Hamazaki, M. Iwabuchi and F. Maekawa, Development and function of bombesin-like peptides and their receptors. Int. J. Dev. Biol. 49 (2005) 293-300
5. N. Minamino, K. Kangawa, and H. Matsuo, Neuromedin B: a novel bombesin-like peptide identified in porcine spinal cord. Biochem. Biophys. Res. Commun. 114 (1983) 541–548.
6. T.J. McDonald, H. Jornvall, G. Nilsson, M. Vagne, M. Ghatei, S.R. Bloom and V. Mutt, Characterization of a gastrin-releasing peptide from porcine non-antral gastric tissue. Biochem. Biophys. Res. Commun. 90 (1979) 227–233.
7. H.C. Weber, Regulation and signaling of human bombesin receptors and their biological effects. Curr. Opin. Endocrinol. Diabetes Obes. 16 (2009) 66–71.
8. R. T. Jensen, J. F. Battey, E. R. Spindel and R. V. Beny, International Union of Pharmacology. LXVIII. Mammalian Bombesin Receptors: Nomenclature, Distribution, Pharmacology, Signaling, and Functions in Normal and Disease States. Pharmacol. Rev. 60 (2008**)** 1-42.
9. R.V. Benya, T. Kusui, T.K. Pradhan, J.F. Battey and R.T. Jensen, Expression and character-ization of cloned human bombesin receptors. Mol. Pharmacol. 47 (1995) 10–20.
10. S. Mahmoud, J. Staley, J. Taylor, A. Bogden, J.–P. Moreau, D. Coy, I. Avis, F. Cuttitta, J. L. Mulshine and T. W. Moody, [Psi13,14] Bombesin analogs inhibit growth of small-cell lung-cancer in vitro and in vivo, Cancer Res. 51 (1991) 1798-1802.
11. Y. Qin, T. Ertl, R-Z Cai, G. Halmos and A. V. Schally, Inhibitory effect of bombesin receptor antagonist rc-3095 on the growth of human pancreatic-cancer cells in-vivo and in-vitro. Cancer Res. 54 (1994) 1035-1041.
12. Z. Merali, J. McIntosh and H. Anisman, Role of bombesin-related peptides in the control of food intake. Neuropeptides. 33 (1999) 376-386.
13. K. Yamada, E. Wada, Y. Santo-Yamada and K. Wada, Bombesin and its family of peptides: prospects for the treatment of obesity. Eur. J. Pharmacol. 440 (2002) 281-290.
14. J.J. Perez, F. Corcho and O. Llorens, Molecular modeling in the design of peptidomimetics and peptide surrogates. Curr. Med. Chem. 9 (2002) 2209-2229.
15. J.J. Perez, Designing Peptidomimetics. Curr. Top. Med. Chem. 18 (2018) 566-590.
16. S. E. Gargosky, J. C. Wallace, F. M. Upton and F. J. Ballard, C-Terminal bombesin sequence requirements for binding and effects on protein synthesis in Swiss 3T3 cells. Biochem. J. 247 (1987) 427-432.

17. J.T. Lin, D.H. Coy, S. A. Mantey and R.T. Jensen, Comparison of the peptide structural requirements for high affinity interaction with bombesin receptors. Eur. J. Pharmacol. 294 (1995) 55-69.
18. M. Broccardo, G. Falconieri Erspamer, P. Melchiorri, L. Negri and R. De Castiglione. Relative Potency of Bombesin-like Peptides. Br. J. Pharmacol. 55 (1975) 221-227.
19. W. Marki, M. Brown and J.E. Rivier. Bombesin Analogs: Effects on Thermoregulation and Glucose Metabolism. Peptides. 2 (1981) 169–177.
20. J. A. Carver, The conformation of bombesin in solution as determined by two-dimensional h-1-nmr techniques, Eur. J. Biochem. 168 (1987) 193-199.
21. J. A. Carver, A two-dimensional H-1-NMR study of the solution conformation of gastrin releasing peptide, Biochem. Biophys. Res. Commun. 150 (1988) 552-560.
22. C. DiBello, L. Gozzini, M. Tonellato, M. G. Corradini, G. D'Auria, L. Paolillo and E. Trivellone, 500 MHz NMR characterization of synthetic bombesin and related peptides in DMSO-D6 by two-dimensional techniques. FEBS Lett. 237 (1988) 85 -90.
23. J. A. Carver, and J. G. Collins, NMR identification of a partial helical conformation for bombesin in solution. Eur. J. Biochem. 187 (1990) 645-650.
24. M. D. DÌaz, M. Fioroni, K. Burger, and S. Berger, Evidence of complete hydrophobic coating of bombesin by trifluoroethanol in aqueous solution: An NMR spectroscopic and molecular dynamics study. Chem. Eur. J. 8 (2002) 1663-1669.
25. D. Erne, and R. Schwyzer, Membrane-structure of bombesin studied by infrared-spectroscopy – prediction of membrane interactions of gastrin-releasing peptide, neuromedin-B, and neuromedin-C. Biochemistry. 26 (1987) 6316-6319.
26. P. Cavatorta, G. Farruggia, L. Masotti, G. Sartor, A. G. Szabo, Conformational flexibility of the hormonal peptide bombesin and its interaction with lipids. Biochem. Biophys. Res. Commun. 141 (1986) 99-105.
27. P. Sharma, P. Singh, K. Bisetty, F.J. Corcho and J.J. Perez, Conformational profile of bombesin assessed using different computational protocols. J. Mol Graph. Model. 29 (2010) 581–590.
28. D.A. Case, T.A. Darden, T.E. Cheatham, III, C.L. Simmerling, J. Wang, R.E. Duke, R.Luo, R.C. Walker, W. Zhang, K.M. Merz, B. Roberts, S. Hayik, A. Roitberg, G. Seabra,J. Swails, A.W. Götz, I. Kolossváry, K.F. Wong, F. Paesani, J. Vanicek, R.M. Wolf, J. Liu,X. Wu, S.R. Brozell, T. Steinbrecher, H. Gohlke, Q. Cai, X. Ye, J. Wang, M.-J. Hsieh, G.Cui, D.R. Roe, D.H. Mathews, M.G. Seetin, R. Salomon-Ferrer, C. Sagui, V. Babin, T.Luchko, S. Gusarov, A. Kovalenko, and P.A. Kollman (2012), AMBER 12, University of California, San Francisco.
29. W. L. Jorgensen, J. Chandrasekhar and J. D. Madura, Comparison of simple potential functions for simulating liquid water. J. Chem. Phys. 79 (1983) 926-935.
30. D. Hamelberg, J. Mongan and J. A. McCammon, Accelerated molecular dynamics: a promising and efficient simulation method for biomolecules. J. Chem. Phys. 120 (2004) 11919-11929.
31. L.C. Pierce, R. Salomon-Ferrer, C. A. F. de Oliveira, J. A. McCammon and R. C. Walker, Routine access to millisecond time scale events with accelerated molecular dynamics. J. Chem.Theory Comput. 8 (2012) 2997-3002.
32. V. Hornak, R. Abel, A. Okur, B. Strockbine, A. Roitberg and C. Simmerling, Comparison of multiple Amber force fields and development of improved protein backbone parameters. Proteins. 65 (2006) 712-725.

33. R. Horst, G. Wider, J. Fiaux, E. B. Bertelsen, A. L. Horwich and K. Wüthrich, Proton–proton Overhauser NMR spectroscopy with polypeptide chains in large structures. Proc. Natl. Acad. Sci. USA. 103 (2006) 15445–15450.
34. J. J. Kuszewski, R. A. Thottungal, C. D. Schwieters and G. M. Clore, Automated error-tolerant macromolecular structure determination from multidimensional nuclear Overhauser enhancement spectra and chemical shift assignments: Improved robustness and performance of the PASD algorithm. J. Biomol. NMR. 41 (2008) 221–239.
35. I. Daidone and A. Amadei, Essential dynamics: Foundation and Applications. WIREs Comput. Mol. Sci. 2 (2012) 762-770.
36. J.J. Perez, M.S.Tomas and J. Rubio-Martinez, Assessment of the sampling performance of multiple-copy dynamics versus a unique trajectory. J. Chem. Inf. Model. 56 (2016)1950-1962
37. J. H. Ward, Hierarchical grouping to optimize an objective function. J. Am. Stat. Assoc. 58 (1963) 236-244.
38. R. W. Newberry and R. T. Raines, Secondary Forces in Protein Folding. ACS Chem. Biol. 14 (2019) 1677−1686.
39. M. Cristau, C. Devin, C. Oiry, O. Chaloin, M. Amblard, N. Bernad, A. Heitz, J.-A. Fehrentz and J. Martinez, Synthesis and Biological Evaluation of Bombesin Constrained Analogues. J. Med. Chem. 43 (2000) 2356-2361.
40. M. Vincenzi, F.A. Mercurio and M. Leone About TFE: Old and New Findings. Curr. Protein Pept. Sci. 20 (2019) 425-451.
41. B. K. Kobilka. G protein coupled receptor structure and activation. Biochim. Biophys. Acta. 1768 (2007) 794–807.

CAPTIONS TO THE FIGURES

Figure 1. Projection of the 400,000 structures selected for the analysis onto their Princial Components. a) Projection onto the three Principal Components PC1-PC3; b) Projection onto components PC1 and PC2. Structures are depicted in colors according to the cluster they belong: cluster#1 red; cluster#2 green; cluster#3 blue; cluster#4 magenta.

Figure 2. Secondary structure adopted by the diverse residues (Y-axis) in the 400,000 structures (X-axis) used for analysis. The color code used is: helix (magenta); turn (blueish-green); extended (yellow). a) Structures of cluster#1; b) Structures of cluster#2; c) Structures of cluster#3; d) Structures of cluster#4.

Figure 3. Structures representing the diverse clusters. (a) Cluster#1; (b) cluster#2; (c) cluster#3; (d) cluster#4.

Figure 4. Contour plot of the Free energy landscape of the peptide. Low regions are plotted in dark blue, whereas high regions in red. The location of the four minima is also indicated.

Figure 5. Structures representing the diverse minima identified in the sampling process. (a) Minimum M1; (b) minimum M2; (c) minimum M3; (d) minimum M4.

Figure 6. Distribution of the distance between the centers of the aromatic rings of the side chains of residues Trp^{8} and His^{12}.

Figure 7. Comparison of the distances deduced from NOEs experiments of bombesin in trifluoethanol/water 30% (v/v) (refs. 23 and 24) and sampled during the whole trajectory of the simulation.

Figure 8. Same as Figure 6 for the distances representing the diverse minima, considering all the structures in the probe square used to draw the FEL of the peptide (Figure 4). (a) Minimum M1; (b) minimum M2; (c) minimum M3; (d) minimum M4.

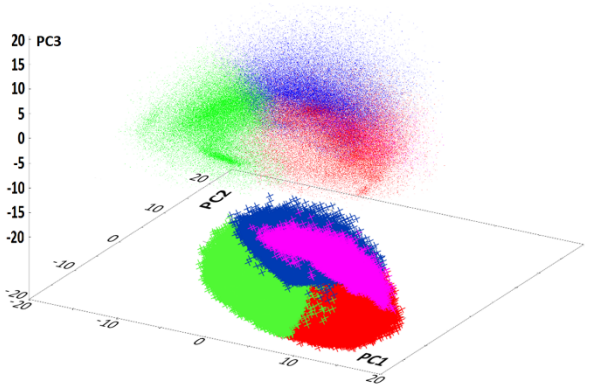

Figure 1

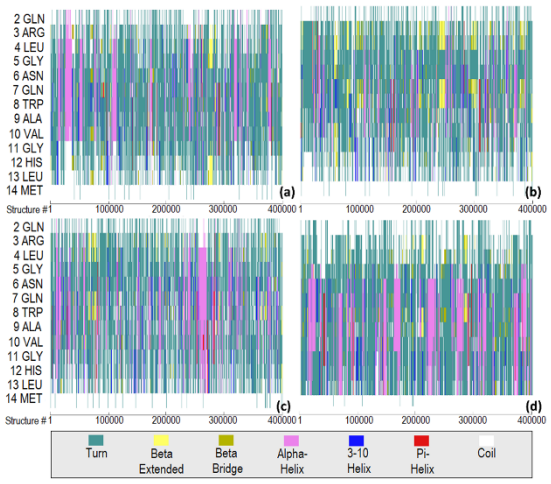
2 GLN
3 ARG
4 LEU
5 GLY
6 ASN
7 GLN
8 TRP
9 ALA
10 VAL
11 GLY
12 HIS
13 LEU
14 MET
(a)
(b)
(c)
(d)
Structure # 1
100000
200000
300000
400000
Turn
Beta Extended
Beta Bridge
Alpha-Helix
3-10 Helix
Pi-Helix
Coil

Figure 2

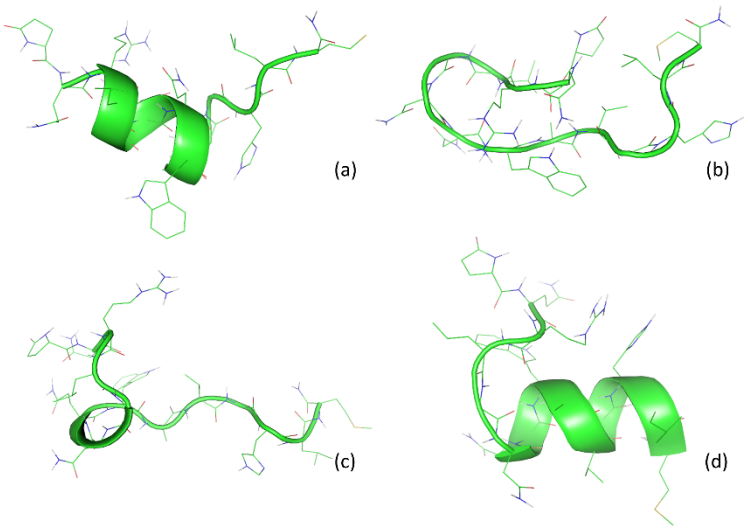

Figure 3

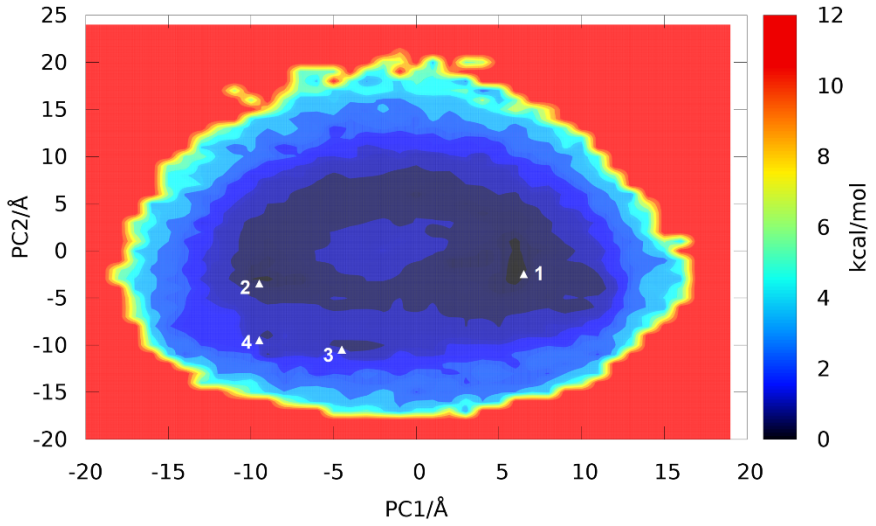
25
20
15
10
5
0
-5
-10
-15
-20
PC2/Å
-20
-15
-10
-5
0
5
10
15
20
PC1/Å
12
10
8
6
4
2
0
kcal/mol
1
2
3
4

Figure 4

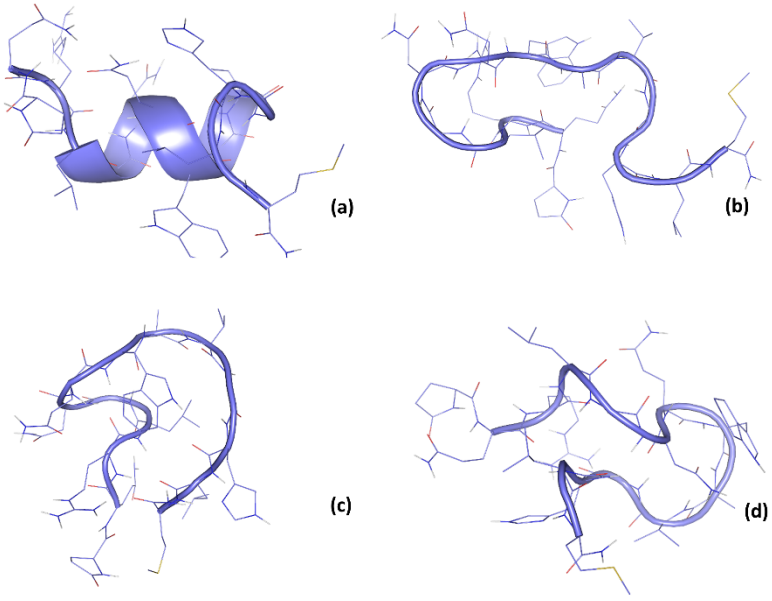

Figure 5

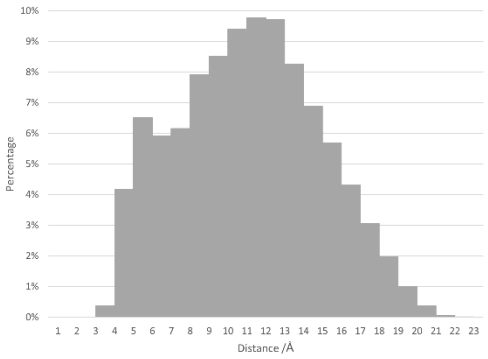
10%
9%
8%
7%
6%
5%
4%
3%
2%
1%
0%
Percentage
1 2 3 4 5 6 7 8 9 10 11 12 13 14 15 16 17 18 19 20 21 22 23
Distance /Å

Figure 6

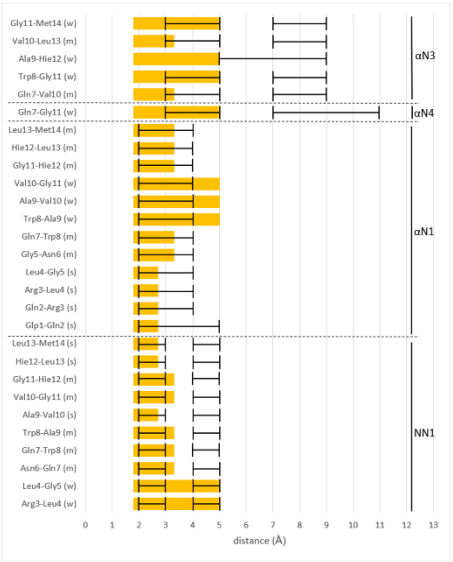
Gly11-Met14 (w)
Val10-Leu13 (m)
Ala9-Hie12 (w)
Trp8-Gly11 (w)
Gln7-Val10 (m)
Gln7-Gly11 (w)
Leu13-Met14 (m)
Hie12-Leu13 (m)
Gly11-Hie12 (m)
Val10-Gly11 (w)
Ala9-Val10 (w)
Trp8-Ala9 (w)
Gln7-Trp8 (m)
Gly5-Asn6 (m)
Leu4-Gly5 (s)
Arg3-Leu4 (s)
Gln2-Arg3 (s)
Glp1-Gln2 (s)
Leu13-Met14 (s)
Hie12-Leu13 (s)
Gly11-Hie12 (m)
Val10-Gly11 (m)
Ala9-Val10 (s)
Trp8-Ala9 (m)
Gln7-Trp8 (m)
Asn6-Gln7 (m)
Leu4-Gly5 (w)
Arg3-Leu4 (w)
αN3
αN4
αN1
NN1
0 1 2 3 4 5 6 7 8 9 10 11 12 13
distance (Å)

Figure 7

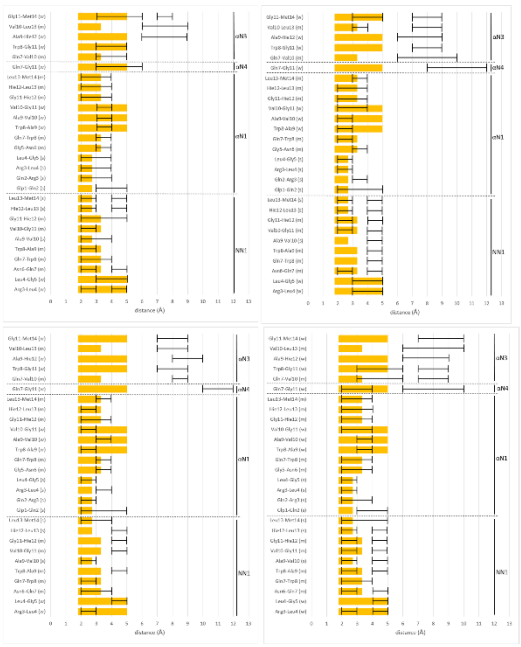

Figure 8